PERGAMON

Deep-Sea Research I 49 (2002) 1195–1216

DEEP-SEA RESEARCH
PART I

www.elsevier.com/locate/dsr

Phytoplankton and iron limitation of photosynthetic efficiency in the Southern Ocean during late summer

Heidi M. Sosik*, Robert J. Olson

Biology Department, Woods Hole Oceanographic Institution, MS 32, Woods Hole, MA 02543-1049, USA

Received 20 August 2001; received in revised form 7 December 2001; accepted 1 March 2002

Abstract

As part of two USJGOFS cruises, we investigated spatial variability in phytoplankton properties across the strong environmental gradient associated with the Antarctic Polar Frontal Zone during late austral summers of 1997 and 1998. Cell properties, including size and an index of pigment content as well as photosynthetic efficiency (as indicated by relative variable fluorescence), changed dramatically across this frontal region. A general trend toward reduced photosynthetic efficiency south of the Polar Front was correlated with low dissolved iron concentration and is consistent with physiological iron limitation in the phytoplankton. We detected no significant differences in photosynthetic efficiency among different size classes of the dominant pico- to nanophytoplankton, despite a systematic community level shift toward larger sized cells south of the Polar Front. In contrast to other cells, those classified as cryptophyte algae showed relatively high photosynthetic efficiency in low iron waters; however, this group was never found in high abundance. One group, all cells $\leqslant 2\,\mu m$, showed an unexpected increase in intracellular pigment content (based on single cell chlorophyll fluorescence measurements) south of the Polar Front where dissolved iron concentration and the cells' relative abundance were low. Overall, these results suggest that group- or size-specific differences in physiological status were not directly regulating community structure in the pico- to nanophytoplankton during the late summer season; other processes, such as differential grazing or sinking losses, must be important.

Keywords: Phytoplankton; Photosynthesis; Fluorescence; Nutrients; Iron; Flow cytometry; Fast repetition rate fluorometry; Southern Ocean; Antarctic Polar Frontal Zone; Ross Sea

1. Introduction

The potential role of iron in regulating Southern Ocean phytoplankton has long been recognized (e.g., Gran, 1931; Harvey, 1933; Hart, 1934; Cooper, 1935), but until recently it was nearly impossible to test directly hypotheses concerning iron effects on phytoplankton physiology, photosynthesis, and growth in natural ecosystems. Renewed interest in assessing the role of iron in marine planktonic ecosystems was sparked by measurements suggesting that vast areas of the open ocean are iron limited (Martin and Fitzwater, 1988) and by results from the first in situ iron enrichment experiments conducted in the Equatorial Pacific, which showed stimulation of phytoplankton physiology and biomass (e.g., Kolber et al., 1994; Martin et al., 1994; Behrenfeld

*Corresponding author. Tel.: +1-508-289-2311; fax: +1-508-457-2134.

E-mail address: hsosik@whoi.edu (H.M. Sosik).

0967-0637/02/$ - see front matter © 2002 Published by Elsevier Science Ltd.
PII: S0967-0637(02)00015-8

et al., 1996; Coale et al., 1996). Synthetic views of how factors such as micronutrient limitation and species-dependent grazing combine to affect the Equatorial Pacific pelagic ecosystem are beginning to emerge (Landry et al., 1997; Leonard et al., 1999). In high latitude regions, potential effects of low iron availability must be considered in the context of seasonal changes in light availability associated with incident solar radiation and deep winter mixing (e.g., Mitchell et al., 1991). For the Southern Ocean, in particular, uncertainty about what combination of factors regulates primary production has important implications for predicting the overall effects of marine processes in global carbon cycling (de Baar et al., 1995; Sarmiento and Le Quere, 1996; Arrigo et al., 1999).

The role of iron in limiting Southern Ocean phytoplankton has been investigated chiefly via iron enrichment experiments in which properties such as chlorophyll, biomass, or physiological parameters are measured over time in control and enriched samples. Because of logistical constraints, these experiments have been almost all shipboard bottle incubations (de Baar et al., 1990; Martin et al., 1990; Buma et al., 1991; Helbling et al., 1991; van Leeuwe et al., 1997; Olson et al., 2000) despite questions about bottle-induced changes in community composition and perturbation of grazing conditions (e.g., Banse, 1991). In situ enrichments, such as those carried out in the Equatorial Pacific (Martin et al., 1994; Coale et al., 1996) and more recently in the Southern Ocean (Boyd et al., 2000), overcome some of the limitations of bottle incubations, and their results have generally agreed with the findings from bottle incubations. Enrichment experiments, however, must be followed for days to document changes; in situ enrichments are especially complex logistically, and even shipboard experiments can be carried out only at selected stations. A realtime in situ assay for iron limitation is needed to overcome these limitations, and active fluorescence techniques may provide the solution.

Active fluorescence approaches (e.g., Falkowski et al., 1992; Olson et al., 1996) for assessing nutritional status of phytoplankton have been used to augment both in situ and bottle enrichment experiments. During in situ enrichment in the Equatorial Pacific (Kolber et al., 1994; Behrenfeld et al., 1996) and the Southern Ocean (Boyd et al., 2000), increases in chlorophyll *a* variable fluorescence were found to precede increases in chlorophyll concentration. Similar relatively rapid physiological responses can occur in bottle incubations with iron enrichment (Olson et al., 2000). Because these responses are so rapid and reflect changes in the status of the photosynthetic machinery (see Falkowski et al., 1992), they are not directly influenced by factors such as changes in grazing pressure that may occur in bottles (e.g., Banse, 1991) and are indicative of physiological limitation.

We previously documented variable fluorescence responses to iron enrichment during post-bloom conditions in late summer for regions of the Ross Sea (Olson et al., 2000); these responses were correlated with the initial level of variable fluorescence: greater increases were observed for cells with lower initial variable fluorescence. In this paper, we examine ambient variable fluorescence and flow cytometry data to document the spatial distribution of iron limiting conditions and associated properties of the phytoplankton. For a transect across the Polar Front, apparent physiological iron limitation is shown to be coincident with the lowest values of dissolved iron concentration observed, but for the Ross Sea a simple correlation with iron concentration is not evident. Over both regions, there was an unexpected inverse correlation between photosynthetic efficiency (as indicated by relative variable fluorescence) and mean phytoplankton cell size. Despite evidence for physiological iron limitation, patterns in phytoplankton biomass and community structure did not appear to be directly related to iron availability at this time of year.

2. Methods

Sampling was conducted in the late summers of 1997 (13 January–11 February) and 1998 (13 February–19 March) as part of the USJGOFS

Antarctic Southern Ocean Process Study (AESOPS). In 1997 (R.V. *Nathaniel B. Palmer* Process II cruise NBP97-1), a series of stations representing an east-west transect across the Ross Sea was occupied twice over 5–6 day periods beginning two weeks apart (stations 1–8 and 13–20); additional stations were located to the north, south, and west of the transect line (Fig. 1). In 1998 (R.V. *Roger Revelle* Process II cruise RR09), we conducted a north–south transect across the Polar Front region; stations were occupied along a section from Christchurch, New Zealand (~43.5°S, 173°E) to 55°S, 170°W and then southward along ~170°W to 71°S. Stations 1–14 represent the southbound transect and 15–30 the northward return transect (Fig. 1). Station data presented here come from a combination of in situ measurements during vertical profiles and analysis of discrete water samples collected from the euphotic zone. In addition to data from vertical profiles at the stations, we also present results from continuous underway sampling of surface water conducted in 1998.

2.1. Station sampling

Vertical profiles were measured with two CTD/rosette systems (a standard plastic-coated rosette with Niskin bottles that had epoxy-coated springs and a "trace metal clean" Teflon-coated rosette with Go-Flo bottles). Ancillary sensors available with the CTD included a bulk chlorophyll fluorometer and a PAR (photosynthetically available radiation, 400–700 nm) sensor. Vertical profiles of active chlorophyll fluorescence assays for photosynthetic properties of phytoplankton were achieved by two approaches. During both cruises, discrete water samples were analyzed on the ship with a PDP ("pump-during-probe") flow cytometer, and, during the Polar Front transect, an in situ FRR ("fast repetition rate") fluorometer was attached to the standard rosette. These two approaches have different advantages: FRR fluorometer measurements can be made with higher space and time coverage than PDP flow cytometry, and PDP flow cytometry allows different groups of phytoplankton to be separately characterized. We have previously shown that these two approaches

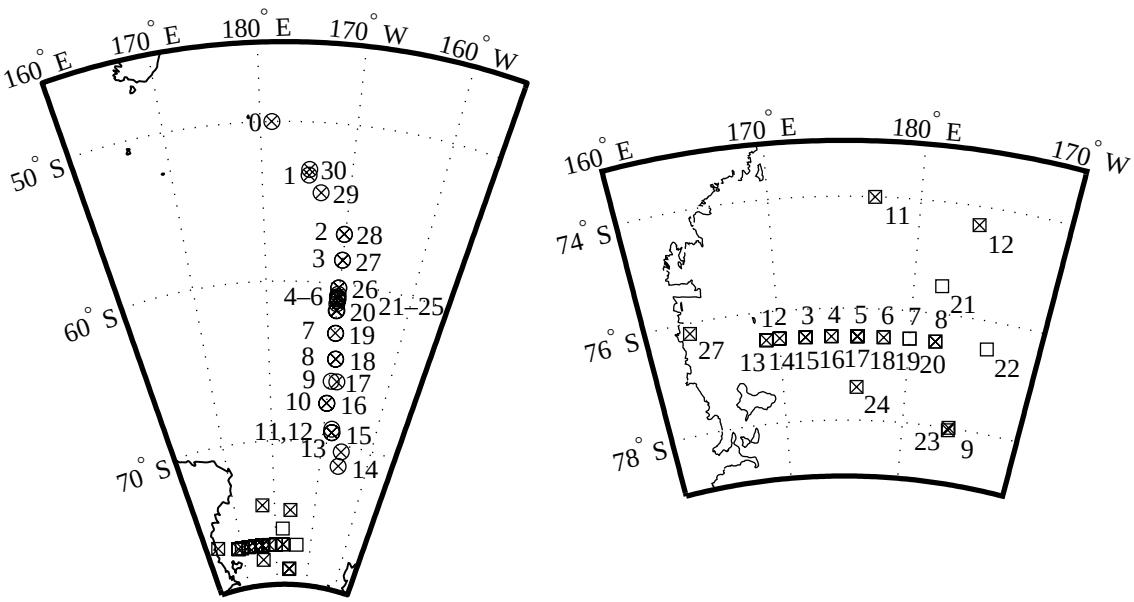

Fig. 1. Locations of stations for which data are presented in this paper (□ = 1997 stations, and ○ = 1998 stations). The right panel is an expanded view of the Ross Sea showing station numbers for sampling in 1997. Stations marked with a cross (X) are those where PDP flow cytometer results are available for 1997, and FRR fluorometer results are available for 1998.

yielded comparable results on the Polar Front cruise (Olson et al., 2000).

Both of these active fluorescence measurements are based on assessment of a fluorescence induction curve over a time scale during which turnover of the photosynthetic reaction centers is negligible. The initial level of fluorescence (F_o) is indicative of the dark-adapted or ambient light condition (depending on the measurement protocol), and the final level of fluorescence (F_m) is achieved after saturation of the photosynthetic reaction centers with the instrument's excitation light. The variable fluorescence ($F_v = F_m - F_o$), when normalized to F_m, is an index of the photochemical conversion efficiency of the phytoplankton being assayed and varies with nutritional status (e.g., Kolber et al., 1988; Greene et al., 1991; Falkowski et al., 1992; Geider et al., 1993). In addition, the photosystem II (PSII) functional absorption cross-section (σ_{PSII}) can be derived from the rate of increase from F_o to F_m given knowledge of the excitation intensity. For the PDP and FRR measurements, F_v/F_m and σ_{PSII} were estimated with slightly different methods as described below.

The PDP flow cytometer, which has been previously described in detail by Olson et al. (1999), allows 150 μs fluorescence induction curves to be measured on each cell as it passes through the flow cytometer. Conventional integrated fluorescence and light scattering signals used to size and identify groups of cells (e.g., Olson et al., 1989) are correlated with each induction curve. From the induction curves, we derived F_v/F_m and σ_{PSII} using non-linear least squares regression to the model proposed by Olson et al. (1996). Water samples were collected in trace metal clean polycarbonate bottles and stored at 2°C before PDP analysis on board the ship; induction curves were measured for individual cells in 0.1–1 ml of seawater. Since induction curves of individual cells are noisy, here we report average fluorescence properties for groups of cells defined by their light scattering and fluorescence cross-sections. Statistical evaluation of differences observed in fluorescence properties among different groups of phytoplankton and across different latitude zones was based on a two-way analysis of variance (5% significance level), followed by a Student–Newman–Keuls Test for means comparison when appropriate.

A battery-powered FRR fluorometer with internal data logging (Chelsea Instruments, Ltd. FAST^{tracka}) was attached at the base of the standard rosette frame and used to collect two types of fluorescence induction curves during vertical profiles. All data presented here are from the instrument's dark chamber, which is enclosed in a black shield; cells assayed in the dark chamber are out of ambient sunlight for ~1 to several seconds depending on the rate of water flow past the instrument. All FRR fluorometer data was collected during downward casts; profiles were typically conducted at 10 m min^{-1} in the first 100 m of the water column and then 40–60 m min^{-1} for the remainder of the cast.

For all of the profiles, excitation conditions in the FRR fluorometer were set to provide 100 flashlets of light (~1 μs duration) spaced ~2.8 μs apart, followed by 20 additional flashlets 50 μs apart. The latter set of flashlets was used to assay the decay of fluorescence yield back to F_o and to estimate reaction center turnover time (τ). This entire sequence of flashlets was repeated at a rate of ~1 s^{-1}, 4 times in the dark chamber alternating with 4 times in the light chamber, and these sets of 4 sequences were averaged to improve signal-to-noise before further processing. To correct for variations in detector response during the 120-flashlet sequence, all fluorescence yields (signals divided by reference measurements of the excitation source) were scaled such that the yield for each flashlet was the same when a standard material with constant fluorescence yield (in this case chlorophyll extracted in methanol) was analyzed. In addition, gain-dependent background signals (estimated from measurements in waters deeper than ~100 m, where fluorescence was below detection) were subtracted from all fluorescence measurements. Although this approach may lead to a blank that is slightly too high or too low depending on effects of background fluorescence levels and depth-dependent changes in light scattering by particles, it is the best estimate available from our measurements. Induction curve parameters (F_v/F_m, σ_{PSII}, and τ) were determined from the model of Kolber et al. (1998) with

software provided by Chelsea Instruments (FRS v. 1.4). All depth profiles of fluorescence properties were smoothed with a 5th order Butterworth low-pass filter with cutoff frequency of 7% of the sample rate. All observations above 10 m were eliminated to avoid any influences of high ambient light, such as contamination of the fluorescence signal by red light from the sun and photoinhibition effects on phytoplankton that persist for more than a few seconds in the dark.

In this paper we also present several other kinds of data acquired from analysis of discrete water samples collected during CTD casts; these data are available at the USJGOFS website (http://usjgofs.whoi.edu). Chlorophyll *a* and macronutrient concentrations were determined by other scientists on the cruises following standard JGOFS protocols (JGOFS, 1996). Micronutrients including dissolved iron were measured by Coale et al. during the 1997 Ross Sea cruise using the method of Johnson et al. (1997) and by Measures and Vink during the 1998 Polar Front cruise using the approach described in Measures et al. (1995). In addition, 5 ml water samples were preserved with 0.1% glutaraldehyde and stored in liquid nitrogen for post-cruise analysis of the abundance, size distribution, and fluorescence of phytoplankton by conventional flow cytometry (Olson et al., 1993). These samples were analyzed with a modified Coulter EPICS flow cytometer in which each optical signal was split and measured by two photomultipliers at different gain settings, which increased the dynamic range of the measurements (allowing cells ranging in size from approximately 1–30 μm to be analyzed simultaneously). All light scattering and fluorescence values, which were measured with logarithmic amplifiers, were converted to linear equivalents and then normalized by the values measured for standard microspheres analyzed in conjunction with the samples (Olson et al., 1993); this provides values in bead units (b.u.) that are comparable between the cruises. Forward light scattering (FLS) was used to estimate cell size through an empirical relationship between FLS and cell volume for a number of marine phytoplankton cultures similar to the approach used by Shalapyonok et al. (2001); the relationship was applied for cells up to 30 μm equivalent spherical diameter. For pennate diatoms, for which FLS underestimates cell volume, chlorophyll fluorescence was used to estimate cell volume assuming the same relationship between fluorescence and volume as other cells in the same sample (Olson et al., 2000). As in Shalapyonok et al. (2001), cellular carbon content was estimated from cell volume and the Eppley et al. (1970) modified Strathmann equation for all nanophytoplankton, and a value of 235 fg C μm^{-3} for *Synechococcus* sp.

Depth-dependent distributions of properties across the Polar Front were produced by interpolation and contouring methods available in the MATLAB software package (Mathworks, Inc.).

2.2. Underway sampling on the Polar Front cruise

Between station work on the 1998 Polar Front cruise, the FRR fluorometer was moved into the ship's laboratory and plumbed with a continuous flow of surface water from the uncontaminated seawater line. During these measurements only the "dark chamber" was activated, but it was necessary to cover the entire sensing head of the instrument (light chamber included) with black optical cloth to prevent room light from reaching the common photodetector. The excitation protocol for these measurements was identical to the one used for the CTD profiles, except that 16 flash sequences were averaged instead of 4 and the final sampling rate (after averaging) for complete induction curves was 2.6 min^{-1}. Statistical evaluation of differences observed in fluorescence properties with time of day and across different latitude zones was based on a two-way analysis of variance with a 5% significance level.

Standard underway measurements of temperature, conductivity, and chlorophyll fluorescence in the uncontaminated seawater flow were made upstream of the FRR fluorometer measurements. In addition, discrete water samples were collected from the uncontaminated seawater flow and analyzed for chlorophyll concentration every 1–2 h, by the same methods as for the water cast samples. The continuous in vivo fluorescence measurements were converted to approximate chlorophyll concentrations based on linear correlation with the

extracted chlorophyll values ($r^2 = 0.56$). It should be noted that fluorometric chlorophyll concentrations yielded higher estimates than those determined by HPLC techniques during this cruise and these differences remain unresolved (Hiscock et al., in press); we report fluorometric values here as an index for general changes in phytoplankton biomass because they were directly associated with the underway sampling.

3. Results

3.1. Bulk variable fluorescence in the upper water column

On neither cruise did we observe average F_v/F_m to approach the expected maximum for nutrient replete growth of $\sim$0.65 (e.g., Kolber et al., 1988; Greene et al., 1992). Average values of F_v/F_m observed with the PDP flow cytometer in the upper 100 m of the Ross Sea in 1997 were spatially variable (Fig. 2A). The highest values were 0.39 at station 27 (nearest to the coast) and 0.34–0.38 at stations 11 and 12 (north of 74.5°); values within the Ross Sea gyre were even lower, between $\sim$0.1 and 0.25 (mean = 0.17, sd = 0.05, $n = 15$ stations). During transects across the Polar Front in 1998, FRR fluorometer observations in the upper 40 m of the water column revealed a distinct transition from relatively high ($> \sim 0.4$) to low values of F_v/F_m that occurred between 61°S and 65°S; the location of the transition may have been further south on the northward transect than on the southward one (Fig. 3A).

During 1998 sufficient FRR fluorometer measurements were made to define patterns of diel variability evident in fluorescence induction properties. Observations from both north and south of 65°S showed a dramatic decrease in F_v/F_m during the daytime (Fig. 4A). In both latitude zones, F_v showed a similar amplitude and pattern of diel variation (Fig. 4B). These patterns arose from variations in both F_o and F_m (not shown). Values of σ_{PSII} also decreased during the day, with greater amplitude in the zone north of 65°S (Fig. 4C). The data for τ was extremely variable but in general values were higher during the day (Fig. 4D). In all cases, there was significant variance associated with time of day ($p \ll 0.001$), but latitude-dependent differences in the relative diel trends (normalized to nighttime values) were significant only for σ_{PSII} ($p \ll 0.001$) and τ ($p = 0.03$).

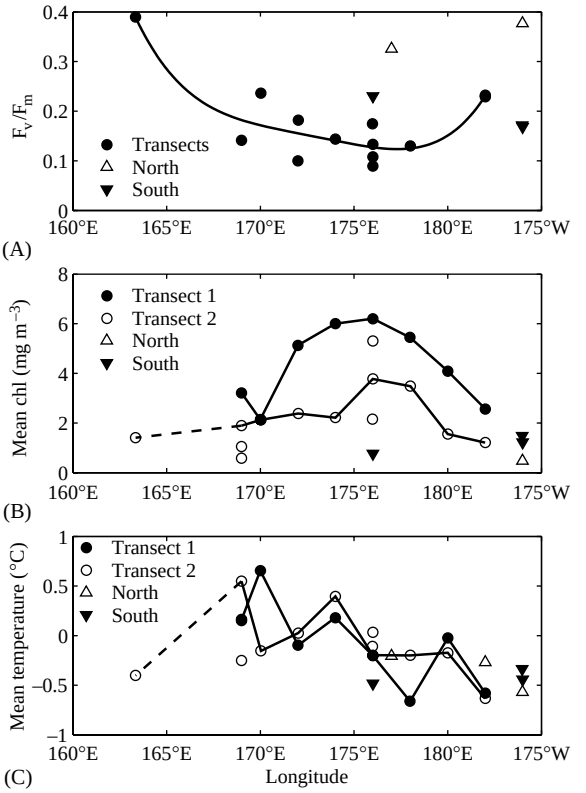

Fig. 2. Mean properties in the upper 40 m of the Ross Sea during late summer 1997. (A) Relative variable fluorescence measured by PDP flow cytometry. (B) Chlorophyll concentration. (C) Water temperature. For temperature and chlorophyll observations, the two consecutive east–west transects are shown separately, with solid lines connecting stations 1–8 and 13–20. For F_v/F_m insufficient measurements were made on the first transect to characterize differences between them, so the observations were pooled and a single trend line presented (least squares fit to a fourth order polynomial). Observations from stations north and south of the main transect line are indicated separately (triangles) in each case, and the pack ice station (27) is included as part of transect 2 despite being occupied 5 days later. F_v/F_m values shown here represent the weighted average of all the phytoplankton sampled by the flow cytometer.

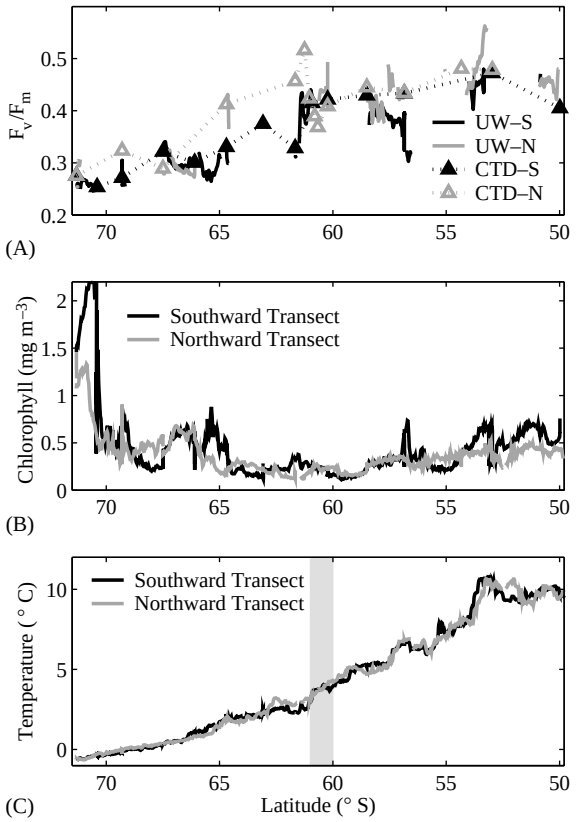

Fig. 3. Surface water properties on the Polar Front transect in 1998. (A) Relative variable fluorescence measured by FRR fluorometry. (B) Chlorophyll concentration derived from underway fluorescence measurements (see text for details). (C) Water temperature. Results from the initial southward transect and the subsequent return north are indicated. All observations were collected during continuous underway analysis of surface seawater, except that average F_v/F_m values for the upper 40 m on CTD casts are also shown (triangles connected by dotted lines in (A)) and underway FRR fluorometer measurements are only shown for nighttime. The approximate location of the Polar Front is indicated in (C).

3.2. Hydrography, nutrients, and chlorophyll

As expected, we observed a much wider range of hydrographic conditions on the Polar Front transect than in the Ross Sea. There were strong latitudinal gradients in temperature and salinity observed on the transect cruise; in the mixed layer temperature ranged from ~ -1°C to 10°C and salinity varied from ~ 33.5 to 34.4, with the lowest values farthest south (Figs. 3C, 5A and B). On the Ross Sea cruise during 1997 variations in surface layer salinities were similar (~ 33.8–34.5), but as expected the temperature range was much smaller (~ -1°C to 1°C; Fig. 2C).

Macronutrients and micronutrients exhibited different patterns of variability, some details of which have been previously described (Gordon et al., 2000; Smith et al., 2000a; Measures and Vink, 2001; Morrison et al., 2001). Macronutrient concentrations varied systematically on the Polar Front cruise, generally increasing towards the south, most dramatically for silicate. Everywhere, except north of 55°S, nitrate and phosphate concentrations exceeded 18 and 1 μM, respectively. An abrupt silicate gradient was present near 65°S by early summer and was still evident in late February; north of this location surface layer concentrations dropped below 10 μM, but southward they consistently exceeded 50 μM (Smith et al., 2000a). Iron concentrations also varied, but in contrast to the macronutrient distributions, dissolved iron concentrations in surface waters were lowest south of ~ 65°S (< 0.15 nM; Fig. 5D; Measures and Vink, 2001). In the Ross Sea during 1997, nitrate was generally > 10 μM, except at station 27, where it dropped as low as 3.5 μM; phosphate was generally > 1 μM and always above 0.5 μM. Surface silicate concentrations were very high: 65–75 μM mid-gyre and 50–60 μM on the northern and western extremes of the study area. Consistent with previous results for summer time in this region (as reviewed by Measures and Vink, 2001), dissolved iron concentrations were low in the Ross Sea surface layer with average concentrations in the upper 100 m < 0.15 nM at all stations, except 3 and 15, where the average was ~ 0.25 nM.

Chlorophyll concentrations were generally indicative of declining or post bloom conditions on both cruises (Smith et al., 2000b; Hiscock et al., in press). On the Polar Front transect, concentrations in surface waters were typically between 0.1 and 0.4 mg m^{-3}, except south of 70°S where they reached 1–2 mg m^{-3} (Fig. 3B). In the Ross Sea, chlorophyll concentrations in the upper 100 m dropped over the month-long cruise from subsurface maxima at the central stations of 7–8 mg m^{-3} in the first week to 3–4 mg m^{-3} by mid-February. In the upper 40 m, concentrations averaged

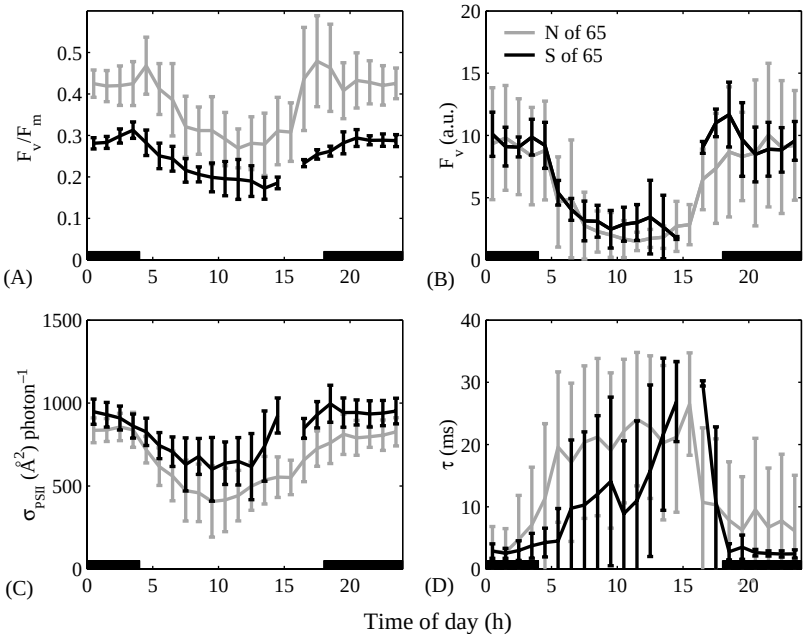

Fig. 4. Diel variations for pooled observations from north and south of 65°S on the Polar Front cruise in 1998. (A) F_v/F_m. (B) F_v. (C) σ_{PSII}. (D) τ. Mean values and standard deviations are shown for 1 h time bins. Time of day is indicated as the local hour, and shaded bars denote the approximate period of nighttime.

between ~2 and 6 mg m^{-3}, with the highest values observed early in the cruise and near the center of the Ross Sea gyre (Fig. 2B).

3.3. Phytoplankton abundance, cell size, pigmentation, and community composition

The abundance and carbon-based biomass of pico- and nanophytoplankton determined by flow cytometry was highest north of 54°S and lowest between 61°S and 65°S (Tables 1 and 2, Figs. 6 and 7). Biomass present south of 69°S was approximately 3-fold higher during the east–west Ross Sea transects than during the north–south Polar Front transects. *Synechococcus*, which were not detected south of ~61°S, were numerically important only north of 55°S and never contributed more than 4% to biomass. *Prochlorococcus* was not present in any samples. Both cryptophytes and pennate diatoms were least abundant between 61°S and 65°S and generally most abundant in the Ross Sea. Cryptophytes never contributed more than a few percent to phytoplankton carbon, but pennate diatoms occasionally contributed nearly half of cell abundance and 20–30% of phytoplankton carbon within the size fraction examined. These diatoms were most important at locations near the periphery of the central Ross Sea gyre (i.e., in the pack ice to the west and at the northernmost stations).

The size distribution of the phytoplankton estimated from flow cytometric analysis showed systematic variation over the region, with a shift from modal diameters <1 μm north of 54°S (due to the presence of *Synechococcus*) to ~3 μm in the Ross Sea for samples from the upper 40 m of the water column (Figs. 8 and 9). Overall variation in size distribution of the phytoplankton was much larger across the Polar Front transect than in the Ross Sea both within and between the cruises. In general, the wide spacing of the peaks in the size distributions indicates that different taxonomic groups dominated in different regions. Within the Ross Sea in 1997, there was an indication that an assemblage of smaller cells (<2 μm) increased in relative abundance during the second east–west

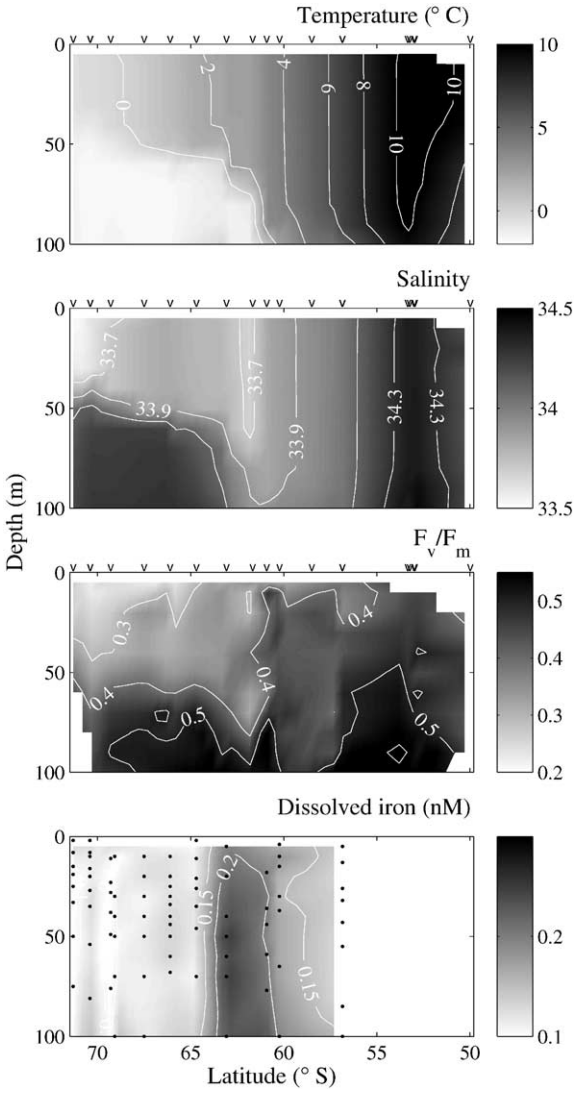

Fig. 5. Contours of interpolated properties on the southward transect during the 1998 Polar Front cruise. (A) Temperature. (B) Salinity. (C) F_v/F_m from dark chamber FRR fluorometer measurements. (D) Dissolved iron. Locations of vertical profiles are indicated at the top of (A), (B), and (C), and discrete sample locations for dissolved iron are indicated in (D). Only data below 10 m depth are shown for F_v/F_m to minimize effects of diel variations evident near the surface (see Fig. 4).

transect through the central Ross Sea gyre; these smaller cells were present north of the east–west transect line, but generally at very low abundance at stations occupied south of the line (Fig. 8). These differences in size distribution are generally reflected in mean diameter for the phytoplankton assemblage, which was lower on the western side of the second transect (Fig. 10A). Across the Polar Front, cells of 1–2 μm diameter were numerically important between 61 and 65°S, with smaller cells increasing in relative abundance to the north and larger cells dominating to the south (Fig. 9). This was reflected in a systematic increase in mean diameter for the entire assemblage with increasing latitude (Fig. 11A). Mean diameters observed south of 65°S in February 1998 were the same as the lowest mean values found in the Ross Sea in early February 1997.

In addition to using the flow cytometric measurements to characterize cell size, we also used the single cell chlorophyll fluorescence measurements to examine changes in intracellular pigment concentration. After normalizing each cell's fluorescence signal to its cell volume, we determined mean values of the ratio for specific size classes of cells. In the upper 40 m of the water column, this ratio of cell fluorescence to cell volume was relatively low and constant for cells between 2 and 5 μm diameter across both the Ross Sea transects and across the Polar Front (Figs. 10C and 11B); the only exception to this generalization was observed near the coast in the pack ice (Ross Sea station 27). For cells smaller than 2 μm, in contrast, cell fluorescence was higher and more variable on both cruises (Figs. 10B and 11B). The highest mean values we observed were on the first Ross Sea transect, and the lowest values occurred in the vicinity of the Polar Front. On the Polar Front transect, in the smallest size classes, there was a dramatic increase in cell fluorescence per volume south of the Front (Fig. 11B).

3.4. Variable fluorescence among phytoplankton groups and size classes

On the basis of PDP flow cytometery measurements, it is possible to examine whether photosynthetic properties differed among groups of cells that can be differentiated by their light scattering and fluorescence properties. Our ability to characterize different cell groups was relatively limited during the Ross Sea sampling in 1997, and we had

Table 1
Mean (standard deviation, number of observations) cell abundances and carbon concentrations for groups of phytoplankton enumerated by flow cytometry on the Ross Sea cruise in 1997. "Total" corresponds to all cells sampled, including the cryptophytes and pennate diatoms. Results are presented for the two east-west transects along 76.5°S and for the groups of stations located north and south of the transect lines

	Station subset			
	Transect 1	Transect 2	Northern	Southern
Cell concentration (ml^{-1})				
Cryptophytes	82 (111, 50)	27 (28, 56)	42 (29, 20)	24 (10, 14)
Pennate diatoms	1244 (1645, 50)	352 (434, 56)	1356 (2265, 20)	894 (701, 14)
Total	7901 (4216, 50)	5021 (3068, 56)	4169 (2845, 20)	4161 (1801, 14)
Carbon ($\mu g l^{-1}$)				
Cryptophytes	5745 (8525, 50)	2889 (6609, 56)	1776 (1163, 20)	691 (294, 14)
Pennate diatoms	9728 (11139, 50)	7260 (13823, 56)	9803 (14823, 20)	6718 (4281, 14)
Total	209255 (68450, 50)	150071 (73322, 56)	98335 (58801, 20)	130373 (30989, 14)

Table 2
Mean (standard deviation, number of observations) cell abundances and carbon concentrations for groups of phytoplankton enumerated by flow cytometry on the Polar Front transect cruise in 1998. "Total" corresponds to all cells sampled, including the *Synechococcus*, cryptophytes, and pennate diatoms. Results are presented for five latitude zones

	Latitude zone				
	$<54°S$	54–61°S	61–65°S	65–69°S	$>69°S$
Cell concentration (ml^{-1})					
Synechococcus	28491 (1543, 5)	794 (901, 45)	22 (33, 31)	2 (3, 18)	0 (1, 29)
Cryptophytes	76 (49, 5)	7 (8, 45)	8 (4, 31)	83 (12, 18)	37 (18, 29)
Pennate diatoms	192 (108, 5)	19 (31, 45)	6 (10, 31)	88 (24, 18)	262 (243, 29)
Total	40932 (1465, 5)	6284 (3676, 45)	2015 (461, 31)	1704 (332, 18)	3756 (711, 29)
Carbon ($\mu g l^{-1}$)					
Synechococcus	2574 (161, 5)	90 (95, 45)	3 (4, 31)	0 (0, 18)	0 (0, 29)
Cryptophytes	1320 (777, 5)	163 (145, 45)	209 (102, 31)	1795 (346, 18)	1202 (693, 29)
Pennate diatoms	844 (499, 5)	83 (150, 45)	132 (455, 31)	548 (149, 18)	1450 (1195, 29)
Total	84718 (23374, 5)	20995 (8780, 45)	13845 (10054, 31)	44003 (15729, 18)	58107 (16404, 29)

some technical problems analyzing large cells (see Olson et al., 2000). We have more detailed observations from the Polar Front cruise and examined latitudinal variations in mean F_v/F_m values for pennate diatoms, cryptophytes, "small" ($<2\,\mu m$) cells, and "large" ($>2\,\mu m$) cells (Fig. 12). Both small and large cells exhibited the same latitudinal trend as the bulk observations from the in situ FRR fluorometer measurements: F_v/F_m was lowest south of 69°S and increased to higher values north of the Polar Front. There were no statistically detectable differences between these size classes ($p > 0.1$). In the southernmost waters, pennate diatoms and especially cryptophytes showed higher values of F_v/F_m than other eukaryotes ($p < 0.001$). Cryptophytes show a statistically significant opposite latitudinal trend from other cells (i.e., higher values further south), despite their low abundance, particularly between 54°S and 65°S (Table 2), and despite the high standard deviations for pooled F_v/F_m values (Fig. 12).

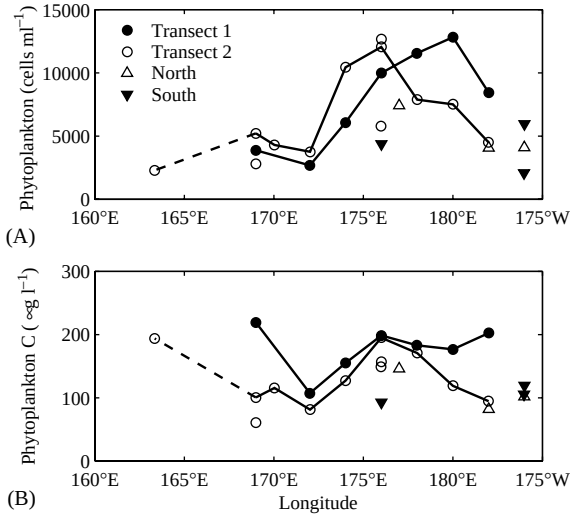

Fig. 6. Mean phytoplankton abundance in (A) and carbon concentration in (B) for the upper 40 m in the Ross Sea, as determined by flow cytometry. As in Fig. 2, results are shown separately for the two east–west transects and for stations north and south of the transect line. Legend in (A) applies to (B) also.

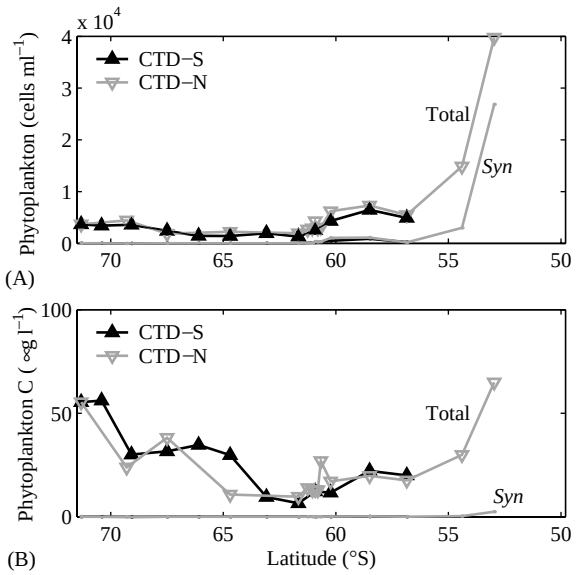

Fig. 7. Mean phytoplankton abundance in (A) and carbon concentration in (B) for the upper 40 m on the Polar Front transect, as determined by flow cytometry. Results are shown for all phytoplankton sampled ("Total") and for cells of the genus *Synechococcus* ("Syn"); they are also separated into the initial southbound set of CTD stations and those on the northbound return.

4. Discussion

4.1. Spatial variability

We observed dramatic differences in photosynthetic efficiency (as indicated by F_v/F_m) and in the size distribution of the phytoplankton community across the complex hydrographic regimes associated with the Pacific sector of the Southern Ocean. During the late summer sampling period, there was an overall trend within the pico- to nanophytoplankton toward larger cell size and lower photosynthetic efficiency with increasing latitude (Figs. 2 and 3). These systematic changes emerged despite substantial mesoscale variability in the region (Abbott et al., 2001; Barth et al., 2001) and in the context of large gradients in temperature, salinity, and concentrations of silicate and iron. The highest gradients in phytoplankton properties occurred in the latitude band between 60°S and 65°S, the zone encompassing the Antarctic Polar Front and the Southern Antarctic Circumpolar Current Front. In this transition zone, seasonal and mesoscale variations appear to be large (Abbott et al., 2000; Morrison et al., 2001), and variability in F_v/F_m and cell size was high even during a single sampling period (Figs. 3 and 11). Within the Ross Sea in 1997, cell size was generally high and F_v/F_m was generally low but with higher values observed near the coast and to the north. The Ross Sea is influenced by a complex set of factors including ice coverage and melting (concentrated at the westernmost edge in summer), shelf water intrusion, and widespread plankton blooms (e.g., Gordon et al., 2000; Smith et al., 2000b). A more extensive set of observations than we currently have will be required to explain the details of meso- to regional scale spatial patterns in photosynthetic efficiency across the Polar Front and in the Ross Sea; in this discussion we concentrate on general latitudinal trends.

4.2. Photosynthetic efficiency and physiological iron limitation

There is a long history of investigation into iron regulation of Southern Ocean phytoplankton (e.g., Gran, 1931; Martin and Fitzwater, 1988; see

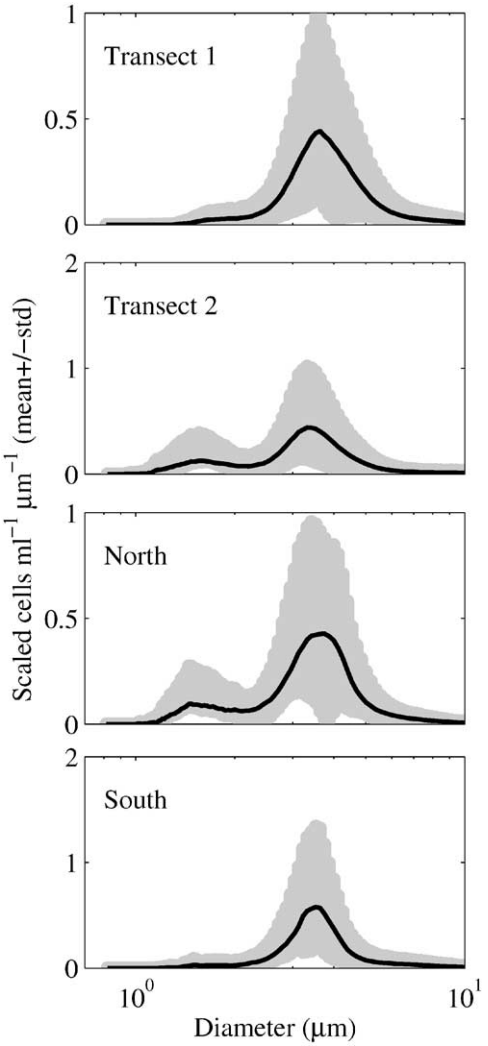

Fig. 8. Mean and standard deviation of the size distribution of phytoplankton in the upper 40 m of the Ross Sea for the same station groups separated in Figs. 2 and 6. Before averaging, each observed size spectrum was scaled to the same concentration of cells to provide indication of changes in shape irrespective of changes in phytoplankton abundance.

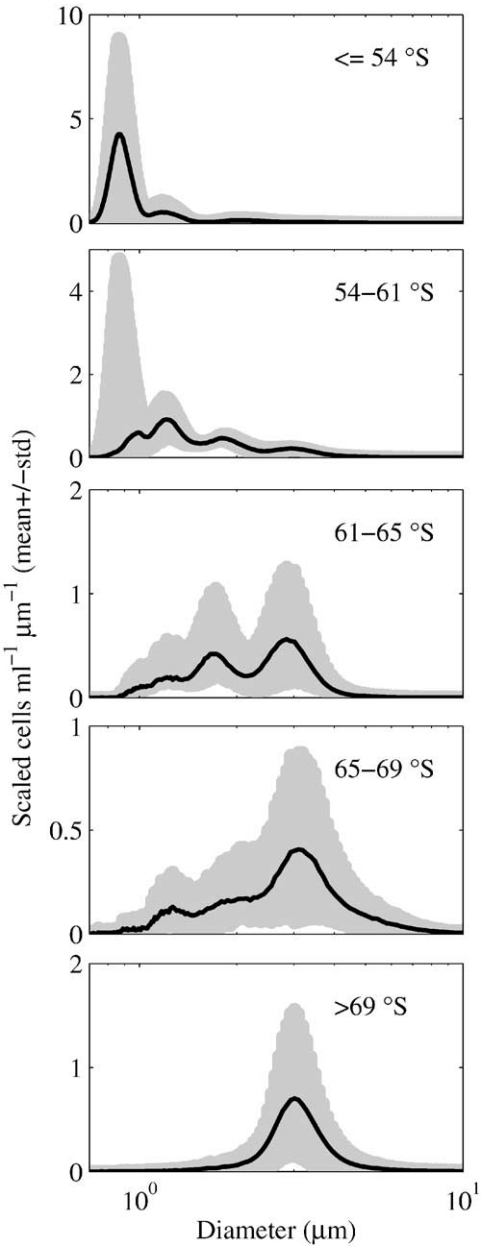

Fig. 9. Mean and standard deviation of the size distribution of phytoplankton in the upper 40 m for latitudinal bands on the Polar Front transect. Observations for the southbound and northbound transects were pooled. As in Fig. 8, each observed size spectrum was scaled to the same concentration of cells to provide an indication of changes in shape irrespective of changes in phytoplankton abundance.

review by de Baar, 1994), but many aspects remain unresolved. As reviewed by Cullen (1991), iron limitation, and nutrient limitation in general, can act at different levels from regulation of aspects of cell physiology to control of standing biomass or rate of productivity. Because our active fluorescence measurements provide a direct assay of

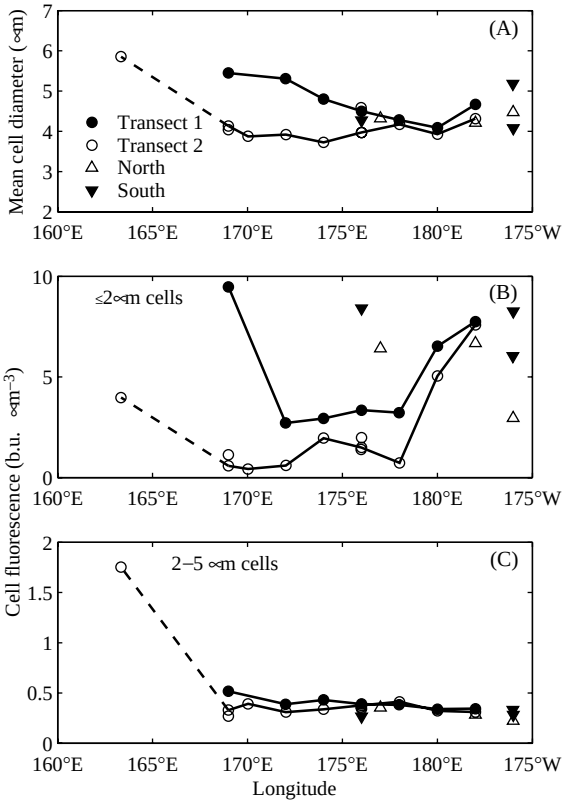

Fig. 10. Mean phytoplankton cell properties for the upper 40 m in the Ross Sea in 1997, as determined by flow cytometry. (A) Mean cell diameter, based on single cell light scattering measurements (see text for details). (B) For cells with diameter $\leqslant 2\,\mu m$, mean single cell chlorophyll fluorescence normalized to cell volume on a cell-by-cell basis, as an index of intracellular pigment concentration. (C) Same as in (B), except for cells with diameter between 2 and 5 μm. For both diameter and fluorescence per cell volume, mean values were first calculated for the assemblage of cells in each discrete sample, and then the means of these values were determined for each station. Note the difference in ordinate scale in (B) and (C), and that the legend in (A) applies to all panels, indicating that results are shown separately for the two east-west transects and for stations north and south of the transect line.

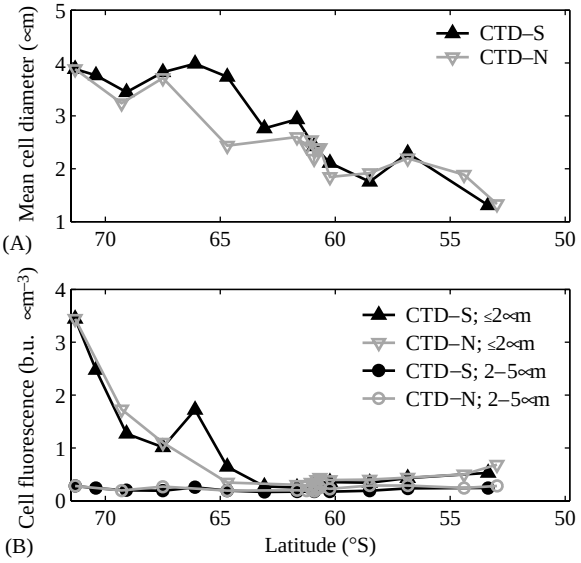

Fig. 11. Mean phytoplankton cell properties for the upper 40 m on the Polar Front transects in 1998, as determined by flow cytometry. (A) Mean cell diameter. (B) Intracellular pigment concentration described by mean single cell chlorophyll fluorescence normalized to cell volume for cells with diameter $\leqslant 2\,\mu m$ and for cells with diameter in the range 2–5 μm. See Fig. 10 for details.

phytoplankton physiological status, we are able to conclude that iron limitation is acting at the level of regulating photosynthetic efficiency, which presumably directly affects cell growth rate.

Our results from the Polar Front cruise in 1998 provide strong evidence for a relationship between the physiological status of the phytoplankton and iron availability. Laboratory studies with marine phytoplankton species have shown that F_v/F_m is expected to decrease when growth rate is low because of limited availability of dissolved iron (Greene et al., 1991, 1992). Response of F_v/F_m values to enrichment of natural waters with iron has also been reported for bottle incubations (Olson et al., 2000) and in situ iron enrichment experiments conducted in the equatorial Pacific (Behrenfeld et al., 1996; Coale et al., 1996) and the Southern Ocean (Boyd et al., 2000). For the upper water column on the Polar Front cruise in 1998, we have shown that F_v/F_m was positively correlated with dissolved iron concentration (Figs. 5 and 13, $r^2 = 0.50$ for all Polar Front data). Although previous studies investigating response to experimental enrichment have supported similar conclusions about iron limitation of phytoplankton, our results provide the first direct evidence of a relationship between ambient dissolved iron concentration and in situ photosynthetic efficiency measured across a natural environmental gradient.

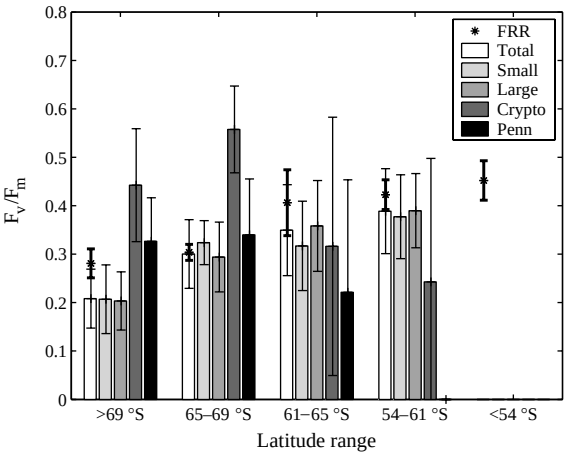

Fig. 12. Mean F_v/F_m values for different phytoplankton groups and size classes based on shipboard PDP flow cytometry on the Polar Front transect. Mean results for the upper 40 m of the water column are shown for "Small" and "Large" size classes (based on light scattering, $\sim 2\,\mu m$ threshold) and for cryptophytes (Crypto) and pennate (Penn) diatoms, both of which can be unambiguously distinguished from other cell types. Corresponding mean values from in situ FRR fluorometry are also indicated (*). Error bars show ± 1 standard deviation for the means. Missing bars correspond to locations where cell concentrations were too low for reliable estimates or, in the case of the $<54°S$, where no samples were collected for PDP analysis.

On the basis of our previously reported relationship between F_v/F_m and response to iron enrichment in the Ross Sea (Olson et al., 2000) and considering the generally low values of F_v/F_m we observed there (Fig. 2A), we believe the Ross Sea was also physiologically iron limited at this time of year. This is consistent with very low phytoplankton growth rates in the Ross Sea during summer (Smith et al., 2000b). The simple relationship between F_v/F_m and iron concentration that we observed across the Polar Front in 1998 was not evident, however, in the results from the 1997 Ross Sea surveys (Fig. 13). It is possible that the lack of correlation between iron concentration and F_v/F_m in this area is due to high frequency (i.e. faster than the physiological response time) variability in dissolved iron concentration or differences in the growth history of the phytoplankton that cannot be explained based on instantaneous nutrient concentration. As suggested by the results of Fitzwater et al. (2000), this region may be complicated by a dynamic pool of particulate iron that is rapidly recycled and spatially variable.

It should be noted that comparison between the two cruises is complicated by the fact that dissolved iron was measured by different methods: the solvent extraction method of Johnson et al. (1997) for the 1997 cruise and the flow injection analysis technique of Measures et al. (1995) for the 1998 cruise. Measures and Vink (2001) have shown that, compared to the method of Johnson et al. (1997), the flow injection analysis technique yielded higher values for dissolved iron in the upper water column during the USJGOFS Polar Front cruise just preceding ours (i.e., in January–February 1998), and they propose that this is due to a greater sensitivity of the flow injection analysis technique to organic fractions of dissolved iron that are important in the upper water column. The correlation between iron concentrations determined with this method and our measurements of F_v/F_m (Fig. 13, Polar Front data only) lends credence to this idea, and further suggests that this iron fraction is accessible to the phytoplankton. During the Ross Sea work in 1997, we observed some relatively high values of F_v/F_m associated with apparently low concentrations of dissolved iron (i.e., stations 11, 12, and 27; see Fig. 13); it is possible that an undetected organic fraction of iron was present in these cases and was accessible to the phytoplankton, thus alleviating severe physiological limitation (station 12 was in fact iron limited as shown by an iron enrichment experiment (Olson et al., 2000)). Two other stations (3 and 15) exhibited an anomaly opposite to the Polar Front cruise trend: apparently high concentrations of dissolved iron and low values of F_v/F_m. These stations were located at 172°E along the east–west transect line, where F_v/F_m was consistently <0.25 (Fig. 2). Surface water dissolved iron concentration was not measured at stations adjacent to 3 and 15, so it is not possible to know if relatively high values were found consistently in this area.

4.3. PSII turnover time and iron limitation

As described by Kolber et al. (1998), the turnover time for PSII can be estimated from

FRR fluorometer measurements of the decay of fluorescence yield after saturation. During our underway sampling across the Polar Front, however, many observations revealed very little decay in fluorescence during the 1.3 ms after saturation, so the reliability of τ values retrieved from the curve fitting procedure was low ($\sim$30% of the observed τ estimates were in excess of 10 ms). If anything, values of τ were lower south of 65° (Fig. 4D), which contradicts expectations for physiological iron limitation. Growth experiments on phytoplankton cultures have documented a systematic increase in τ with increasing iron limitation (Greene et al., 1992), and τ decreased following iron addition to a patch of water in the Equatorial Pacific (Kolber et al., 1994); these results contrast with the apparent absence of an effect on τ of nitrogen limitation based on laboratory work (Kolber et al., 1988).

Falkowski et al. (1992) have proposed that, for natural samples, this contrast in how τ responds can be used as the basis for discriminating between the physiological effects of nitrogen and iron limitation, both of which may result in reduced F_v/F_m. We observed a latitudinal decrease in F_v/F_m without an increase in τ, so on the basis of these simple criteria our results appear consistent with physiological nitrogen limitation. As discussed above, the conclusion that the phytoplankton in waters south of 65°S were physiologically nitrogen limited is strongly refuted, however, by the results of bottle enrichment experiments (Olson et al., 2000) and is inconsistent with the very high concentration of nitrate observed in these waters on our cruise. The iron enrichment experiments we conducted north of $\sim$65°S showed no effect of iron, but those farther south showed an increase in F_v/F_m compared to controls that was evident by the first sampling point at $\sim$48 h (Olson et al., 2000). As Falkowski et al. (1992) proposed, it is possible that consistently high τ values will be found in the Southern Ocean due to low temperatures, regardless of nutrient availability. These findings suggest that substantial work will be required to adequately interpret natural patterns of variability in PSII turnover time from FRR fluorometer measurements; results from laboratory studies of a few species cannot be simply extrapolated to natural conditions, and we will continue to rely on supporting evidence from experimental procedures like enrichment incubations for accurate interpretation of fluorescence properties.

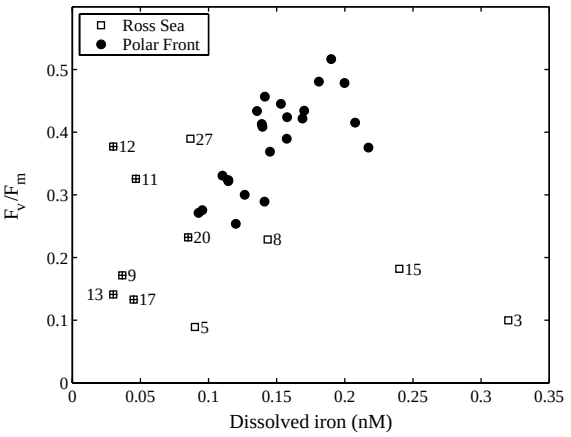

Fig. 13. Relationships between F_v/F_m and dissolved Fe concentration for both cruises. All values are the mean of observations in the upper 40 m of the water column, except for iron in the Ross Sea, where 60 m was used (because there was often only one measurement in the top 40 m). F_v/F_m values were derived from all cells measured by PDP flow cytometry in the Ross Sea and from in situ FRR measurements on the Polar Front transect. Station numbers are noted to the right of data points for the Ross Sea (see Fig. 1), and stations with one or more iron value at or below the detection limit of 0.03 nM are also indicated (+). For the Polar Front transect, $r^2 = 0.50$.

4.4. Diel variations in photosynthetic properties

In surface waters, we observed dramatic diel variations in photosynthetic efficiency and in the absorption cross-section for PSII in all regions we sampled (Fig. 4A and C). Generally values of F_v/F_m and σ_{PSII} were lowest during the mid-day hours and higher at night. These patterns were similar for both iron-limited cells and for cells in waters where iron limitation was not apparent (i.e., north of 65°S). These changes are consistent with natural sunlight causing photoinhibitory effects that require several minutes or longer for recovery. Behrenfeld and Kolber (1999) reported a similar diel pattern for F_v/F_m in the central Atlantic gyres, but an opposite day–night trend

in the South Pacific, which they propose is indicative of iron limitation in these waters; they also observed a strong nighttime depression in σ_{PSII} in the Pacific that was absent in the Atlantic. Their explanation for these differences in diel patterns is based on the particular physiological response to iron limitation of picoplanktonic cyanobacteria, which dominate the phytoplankton community in the oligotrophic gyres. Since our flow cytometric observations showed that cyanobacteria were not present south of 60°S (Fig. 7, Table 2), we would not expect to see evidence of a change in diel pattern across the transect associated with iron limitation in the southern waters (Fig. 4A). Interestingly, absolute diel changes in F_v were almost indistinguishable between the two latitude zones we examined (Fig. 4B), and Behrenfeld and Kolber (1999) report relative diel changes in F_v that were the same for the Atlantic and the Pacific.

4.5. Control of biomass

Since photosynthetic efficiency should be related to growth rate, we would expect areas with high F_v/F_m to be increasing in biomass. At any particular sampling time, however, the relationship between standing stock of biomass and F_v/F_m cannot be expected to be simple because standing stock will depend on the history of resource availability, production, and losses. In fact, for our late summer sampling, we did not observe a simple pattern of high biomass associated with high F_v/F_m. Average F_v/F_m values were very low in the Ross Sea surface waters, yet total chlorophyll *a* concentration, and pico- and nanophytoplankton abundance and carbon concentration were generally the highest observed. During the Polar Front transect we observed higher concentrations of chlorophyll (Fig. 3B) and phytoplankton carbon (Fig. 7B) south of 65°S compared with 60–65°S, but F_v/F_m was higher at the northern latitudes (Fig. 5). These results indicate that latitudinal differences in phytoplankton physiology driven by iron availability in late summer cannot directly explain observed differences in standing stock of phytoplankton. Not surprisingly, other factors must be considered to explain spatial patterns in biomass at this time of year.

The availability of micro- and macronutrients has proven useful for explaining some aspects of seasonal-scale changes in phytoplankton biomass in this region (Smith et al., 2000b; Landry et al., 2002; Hiscock et al., in press), but light and nutrient history, as well as the rates of cell loss processes such as grazing and sinking, must also be considered (Abbott et al., 2000). A likely contributing factor to the biomass differences we observed is related to loss processes and the composition of the plankton community earlier in the season. In the Ross Sea, *Phaeocystis antarctica* tends to be important during the spring bloom (Arrigo et al., 1999; Caron et al., 2000); this species, which does not sink rapidly and, during its colonial life stage, may evade grazing by protozoa, was still present during our summertime sampling. Moreover, Caron et al. (2000) reported that microzooplankton grazing rates were always low relative to phytoplankton growth rates during spring-summer 1996–1997 in the Ross Sea. In contrast, large diatoms, which typically sink rapidly once nutrients are depleted, dominated during the bloom in the Polar Front region, but were not present in high abundances in late summer north of 65°S (Landry et al., 2002). In addition, the impact of microzooplankton grazing was high in this region (Landry et al., 2001; Landry et al., 2002).

4.6. Phytoplankton cell size, pigmentation, and community composition

It may not be surprising that the spatial patterns of phytoplankton biomass in late summer were not a simple function of iron concentration, but we did expect that cell properties such as size and intracellular pigment concentration would reflect physiological effects of iron limitation. Interestingly, we observed two spatial patterns in the properties of the pico- to nanophytoplankton that are inconsistent with previous studies of effects of iron limitation under laboratory conditions and during enrichment experiments with natural assemblages.

The first of these relates to cell size, which we have used as an index for community structure. The current paradigm is that cells of small size dominate the phytoplankton community under iron limiting conditions, and that large cells are important contributors to phytoplankton biomass only if nutrients are present at elevated concentrations. An important line of evidence for this generalization comes from in situ enrichment experiments during which all cell types were observed to respond to iron enrichment, but the relative abundance of large diatoms increased dramatically (e.g., Kolber et al., 1994; Coale et al., 1996; Cavender-Bares et al., 1999; Gall et al., 2001). Diffusion limitation of nutrient uptake may be significant for large cells, and both experimental and theoretical work supports the idea that small cells will be favored under nutrient limiting conditions (e.g., Raven, 1986; Morel et al., 1991; Chisholm, 1992; Sunda and Huntsman, 1997). On the basis of these views and the patterns in iron concentration and F_v/F_m that we observed, we expected that phytoplankton cell size would generally have decreased with increasing latitude across the Polar Front region and into the Ross Sea. Instead, for the pico- to nanophytoplankton, we observed systematic increases in mean diameter with increasing latitude (Fig. 11A) indicative of shifts in the community composition (Fig. 9). The Ross Sea observations from 1997, which were farther south than any of the measurements on the Polar Front transect, showed the largest cell size (Fig. 8 and 10A). The result of these observations is that we observed an inverse correlation between mean cell size and our primary indicator of physiological status, F_v/F_m (Fig. 14).

Given the apparent iron limiting conditions south of 65°S, the second unexpected trend in cell properties was the increase in cellular fluorescence we observed in these waters. Cells exposed to iron limiting growth conditions in the laboratory exhibit low intracellular chlorophyll concentration (reviewed by Geider and La Roche, 1994). Consistent with these observations, during iron enrichment experiments in the equatorial Pacific flow cytometry revealed increases in chlorophyll fluorescence per cell for all cell types examined, including picophytoplankton and pennate diatoms

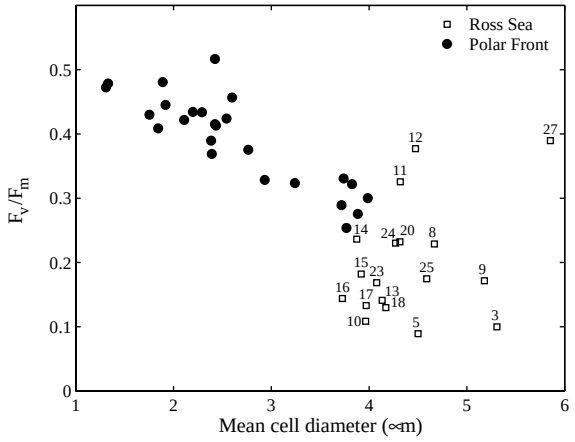

Fig. 14. Relationships between F_v/F_m and mean phytoplankton cell size for both cruises. All values are the mean of observations in the upper 40 m of the water column. As in Fig. 10, F_v/F_m values were derived from all cells measured by PDP flow cytometry in the Ross Sea and from in situ FRR measurements on the Polar Front transect. Station numbers are noted to the right of data points for the Ross Sea cruise (see Fig. 1). Overall $r^2 = 0.58$; for the Polar Front transect only, $r^2 = 0.75$.

(Zettler et al., 1996; Cavender-Bares et al., 1999). In addition, Gall et al. (2001) reported increases in chlorophyll *a* per cell during the SOIREE in situ iron enrichment in the Antarctic Polar Front region. On the basis of these observations, we expected that pigment per cell would be low for cells south of 65°S, but our flow cytometry results do not support this.

Since we observed dramatic changes in cell size distribution across the Polar Front, we normalized our cell fluorescence measurements to cell volume to examine intracellular chlorophyll concentrations. Instead of the predicted decrease in chlorophyll fluorescence per cell volume with increasing latitude (and decreasing iron concentration), we observed little or no change in cells larger than 2 μm and an increase in the smallest cells, $\leqslant 2\,\mu m$ (Fig. 11B); the highest values observed were for small cells in the Ross Sea in 1997 (Fig. 10). Interestingly, even though the smallest cells showed no signs of low iron leading to decreased pigmentation in the southernmost waters (Fig. 11B), their contribution to the community

decreased dramatically (Table 2 and Fig. 9). Increases in pigment per cell can also be caused by factors other than nutrient limitation such as decreases in light availability (e.g., Falkowski et al., 1985) and increases in growth temperature (e.g., Sosik and Mitchell, 1994). For this dataset, however, both light and temperature changes might be expected to lead to decreased pigment per cell with increasing latitude. Mixed layer light levels were likely to be lower north of the Polar Front (mixed layer depths were deeper than the critical depth) compared to south of it (where the mixed layer was shallower than the critical depth) (Hiscock et al., in press); and mixed layer temperatures decreased with increasing latitude (Fig. 3).

A possible explanation for the observation that pigment per cell did not decrease as iron limitation increased is that, even within a limited size class (e.g., $\sim$1–2 μm cells), there are systematic changes in species composition across this strong environmental gradient, and these changes obscure simple expectations about cell properties based on our knowledge of phytoplankton physiology and nutrient limitation. These results suggest that characterization of species level shifts in the community and the factors that regulate community structure in these waters must be better understood before we can explain patterns of variability in properties such as cell pigmentation.

4.7. Group- and size-specific photosynthetic efficiency

There was a notable exception to the generalization that F_v/F_m was low south of 65°S; in low iron waters where all other cell types exhibited depressed F_v/F_m, cryptophyte algae had relatively high values. This result parallels our observations of the response to iron enrichment for this group, which was always lower than for other cells (Olson et al., 2000), and suggests that they are somehow able to avoid the physiological effects of iron stress. As we proposed previously (Olson et al., 2000), it is possible that they accomplish this through mixotrophy, with phagocytosis providing an additional source of iron not generally available to other photosynthetic cells. Regardless of the mechanism, however, given its apparently high photosynthetic efficiency in the areas south of 65°S, it is unclear why this group of cells never constituted a large fraction of the phytoplankton biomass. There must have been a significant group-specific loss term, such as targeted grazing, that prevented them from blooming or increasing dramatically in relative abundance.

Consistent with other evidence of the seasonal shifts in phytoplankton community structure in this region (Landry et al., 2002), we observed relatively few pennate diatoms in late summer, although along the edges of the Ross Sea gyre they occasionally contributed significantly to carbon biomass. On the Polar Front transect, this group of cells had low F_v/F_m and low abundance, most likely due to a combination of iron limitation that affected all groups (except cryptophytes) south of $\sim$65°S and to silica limitation preventing their growth in more northern waters (Franck et al., 2000). Interestingly, for reasons we cannot explain, this group did exhibit significantly higher than average F_v/F_m values in the southernmost waters of the transect (Fig. 12).

Cryptophytes and pennate diatoms, the two groups of phytoplankton we could reliably discriminate from our flow cytometric light scattering measurements, accounted for only a small fraction of the total phytoplankton biomass. When we examined the distribution of F_v/F_m in the rest of the pico- and nanoplankton by grouping the cells according to size, we found that F_v/F_m of small and large cells in a given region were never significantly different. Even though we observed latitudinal changes in phytoplankton size distributions, these changes were apparently not linked to size-related differences in photosynthetic properties. The shift favoring the larger cells towards the south was not associated with their being better off physiologically compared to the small cells; both groups were physiologically impaired in the south (Fig. 12). This finding is consistent with results from in situ iron enrichment experiments, where F_v/F_m has been reported to increase for all size classes in the equatorial Pacific (Kolber et al., 1994) and in the Southern Ocean (Boyd and Abraham, 2001). Because so few species have been characterized in laboratory studies, we must

consider the possibility that the relationship between iron limitation and F_v/F_m is species or size-dependent; this would complicate the interpretation of F_v/F_m for natural assemblages. In the absence of such complicating factors, our results suggest that the dominance of relatively large (2–5 μm) cells in the southernmost waters we sampled is not simply due to greater photosynthetic efficiency under low iron conditions, and leads to the conclusion that other factors must be critical for regulating community structure across this region at this time of year.

5. Conclusions

On the basis of in situ and single cell assessment of fluorescence properties, we have reported evidence of physiological iron limitation south of the Antarctic Polar Front in late summer. During a north–south transect of the region, low photosynthetic efficiency was correlated with low dissolved iron concentration, although the relationship was more complicated in the Ross Sea. In contrast to expectations, we found larger cell sizes in the pico- to nanophytoplankton in the low iron waters, despite larger cells having photosynthetic efficiency that was just as low as the small cells, and small cells showing no indication of low iron effects such as pigment loss.

To our knowledge, there have been no laboratory studies investigating variations in fluorescence-derived photosynthetic properties for cold-water species under different light and nutrient conditions. As long as our information from controlled studies is limited to relatively large temperate water species, interpretation of observations across natural environmental gradients at high latitudes will remain problematic. In any case, for accurate characterization of effects of nutrient limitation on phytoplankton growth, biomass, and productivity, we will continue to rely on combinations of highly resolved measurements, such as those from in situ FRR fluorometers, and more detailed measurements from discrete samples, including monitoring of responses to experimental manipulations and monitoring of group-, species- and size-specific properties.

Despite evidence of physiological iron limitation, we found no indication that differences in physiological capability led directly to differences in use of available resources, and ultimately to spatial patterns in standing stock and community composition during late summer in the Pacific sector of the Southern Ocean. The physiological status of the phytoplankton is only one piece of this puzzle, and, not surprisingly, other factors such as loss processes, including grazing and sinking, and the history of growth and losses occurring earlier in the season must be important in determining spatial patterns in phytoplankton community structure, biomass, and productivity.

Acknowledgements

We wish to thank Alexander Chekalyuk and Alexi Shalapyonok for help with data collection. We are also indebted to the researchers of the AESOPS program for sharing data, especially Chris Measures and Kenneth Coale for results on dissolved iron concentrations. This work was supported by NSF grant OPP-9530718 to RJO and HMS and by NASA grant NAG5-7538 to HMS. This is Woods Hole Oceanographic Institution contribution number 10509.

References

Abbott, M.R., Richman, J.G., Letelier, R.M., Bartlett, J.S., 2000. The spring bloom in the Antarctic Polar Frontal Zone as observed from a mesoscale array of bio-optical sensors. Deep-Sea Research II 47, 3285–3314.

Abbott, M.R., Richman, J.G., Nahorniak, J.S., Barksdale, B.S., 2001. Meanders in the Antarctic Polar Frontal Zone and their impact on phytoplankton. Deep-Sea Research II 48, 3891–3912.

Arrigo, K.R., Robinson, D.H., Worthen, D.L., Dunbar, R.B., DiTullio, G.R., VanWoert, M., Lizotte, M.P., 1999. Phytoplankton community structure and the drawdown of nutrients and CO_2 in the Southern Ocean. Science 283, 365–367.

Banse, K., 1991. Rates of phytoplankton cell division in the field and in iron enrichment experiments. Limnology and Oceanography 36, 1886–1898.

Barth, J.A., Cowles, T.J., Pierces, S.D., 2001. Mesoscale physical and bio-optical structure of the Antarctic Polar

Front near 170°W during austral spring. Journal of Geophysical Research 106, 13879–13902.

Behrenfeld, M.J., Kolber, Z.S., 1999. Widespread iron limitation of phytoplankton in the South Pacific Ocean. Science 283, 840–843.

Behrenfeld, M.J., Bale, A.J., Kolber, Z.S., Aiken, J., Falkowski, P.G., 1996. Confirmation of iron limitation of phytoplankton photosynthesis in the Equatorial Pacific Ocean. Nature 383, 508–511.

Boyd, P.W., Abraham, E.R., 2001. Iron-mediated changes in phytoplankton photosynthetic competence during SOIREE. Deep-Sea Research II 48, 2529–2550.

Boyd, P.W., Watson, A.J., Law, C.S., Abraham, E.R., Trull, T., Murdoch, R., Bakker, D.C.E., Bowie, A.R., Buesseler, K.O., Chang, H., Charette, M., Croot, P., Downing, K., Zeldis, J., et al., 2000. A mesoscale phytoplankton bloom in the polar Southern Ocean stimulated by iron fertilization. Nature 407, 695–702.

Buma, A.G.J., De Baar, H.J.W., Nolting, R.F., van Bennekom, A.J., 1991. Metal enrichment experiments in the Weddell-Scotia Seas: effects of Fe and Mn on various plankton communities. Limnology and Oceanography 36, 1865–1878.

Caron, D.A., Dennett, M.R., Lonsdale, D.J., Moran, D.M., Shalapyonok, L., 2000. Microzooplankton herbivory in the Ross Sea, Antarctica. Deep-Sea Research II 47, 3249–3272.

Cavender-Bares, K.K., Mann, E.L., Chisholm, S.W., Ondrusek, M.E., Bidigare, R.R., 1999. Differential response of equatorial Pacific phytoplankton to iron fertilization. Limnology and Oceanography 44, 237–246.

Chisholm, S.W., 1992. Phytoplankton size. In: Falkowski, P.G., Woodhead, A.D. (Eds.), Primary Productivity and Biogeochemical Cycles in the Sea. Plenum, New York, pp. 213–237.

Coale, K.H., Johnson, K.S., Fitzwater, S.E., Gordon, R.M., Tanner, S., Chavez, F.P., Ferioli, L., Sakamoto, C., Rogers, P., Millero, F., Steinberg, P., Nightingale, P., Cooper, D., Cochlan, W.P., Kudela, R., 1996. A massive phytoplankton bloom induced by an ecosystem-scale iron fertilization experiment in the Equatorial Pacific Ocean. Nature 383, 495–501.

Cooper, L.H.N., 1935. Iron in the sea and in marine phytoplankton. Proceedings of the Royal Society of London Series B-Biological Sciences 118, 419–438.

Cullen, J.J., 1991. Hypotheses to explain high-nutrient conditions in the open sea. Limnology and Oceanography 36, 1578–1599.

de Baar, H.J.W., 1994. Von Liebig's Law of the Minimum and plankton ecology (1899–1991). Progress in Oceanography 33, 347–386.

de Baar, H.J.W., Buma, A.G.J., Nolting, R.F., Cadee, G.C., Jacques, G., Treguer, P.J., 1990. On iron limitation in the Southern Ocean: experimental observations in the Weddell and Scotia Seas. Marine Ecology Progress Series 65, 105–122.

de Baar, H.J.W., de Jong, J.R.M., Bakker, D.C.E., Loscher, B.M., Veth, C., Bathmann, U., Smetacek, V., 1995. Importance of iron for plankton blooms and carbon dioxide drawdown in the Southern Ocean. Nature 373, 412–415.

Eppley, R.W., Reid, F.M.H., Strickland, J.D.H., 1970. Estimates of phytoplankton crop size, growth rate and primary production off La Jolla, CA in the period April through September 1967. In: Strickland, J.D.H. (Ed.), Bulletin of the Scripps Institution of Oceanography, Vol. 17. University of California Press, Berkeley, CA, pp. 33–42.

Falkowski, P.G., Dubinsky, Z., Wyman, K., 1985. Growth-irradiance relationships in phytoplankton. Limnology and Oceanography 30, 311–321.

Falkowski, P.G., Greene, R.M., Geider, R.J., 1992. Physiological limitations on phytoplankton productivity in the ocean. Oceanography 5, 84–91.

Fitzwater, S.E., Johnson, K.S., Gordon, R.M., Coale, K.H., Smith Jr., W.O., 2000. Trace metal concentrations in the Ross Sea and their relationship with nutrients and phytoplankton growth. Deep-Sea Research II 47, 3159–3179.

Franck, V.M., Brzezinski, M.A., Coale, K.H., Nelson, D.M., 2000. Iron and silicic acid concentrations regulate Si uptake north and south of the Polar Frontal Zone in the Pacific Sector of the Southern Ocean. Deep-Sea Research II 47, 3315–3338.

Gall, M.P., Boyd, P.W., Hall, J., Safi, K.A., Chang, H., 2001. Phytoplankton processes. Part 1: Community structure during the Southern Ocean Iron RElease Experiment (SOIREE). Deep-Sea Research II 48, 2551–2570.

Geider, R.J., La Roche, J., 1994. The role of iron in phytoplankton photosynthesis, and the potential for iron-limitation of primary productivity in the sea. Photosynthesis Research 39, 275–301.

Geider, R.J., La Roche, J., Greene, R.M., Olaizola, M., 1993. Response of the photosynthetic apparatus of *Phaeodactylum tricornutum* (Bacillariophyceae) to nitrate, phosphate, or iron starvation. Journal of Phycology 29, 755–766.

Gordon, L.I., Codispoti, L.A., Jennings Jr., J.C., Millero, F.J., Morrison, J.M., Sweeney, C., 2000. Seasonal evolution of hydrographic properties in the Ross Sea, Antarctica, 1996–1997. Deep-Sea Research II 47, 3095–3117.

Gran, H.H., 1931. On the conditions for the production of plankton in the sea. Rapports et procès-verbaux des réunions. Conseil Permanent International pour L'Exploration de la mer 75, 37–46.

Greene, R.M., Geider, R.J., Falkowski, P.G., 1991. Effect of iron limitation on photosynthesis in a marine diatom. Limnology and Oceanography 36, 1772–1782.

Greene, R.M., Geider, R.J., Kolber, Z., Falkowski, P.G., 1992. Iron-induced changes in light harvesting and photochemical energy conversion processes in eukaryotic marine algae. Plant Physiology 100, 565–575.

Hart, T.J., 1934. On the phytoplankton of the south-west Atlantic and the Bellingshausen Sea, 1929–1931. Discovery Reports 8, 1–286.

Harvey, H.W., 1933. On the rate of diatom growth. Journal of the Marine Biological Association of the UK 19, 253–276.

Helbling, E.W., Villafane, V., Holm-Hansen, O., 1991. Effect of iron on productivity and size distribution of Antarctic phytoplankton. Limnology and Oceanography 36, 1879–1885.

Hiscock, M., Marra, J., Smith, W.O., Jr., Goericke, R., Measures, C., Vink, S., Olson, R.J., Sosik, H.M., Barber, R.T. Primary productivity and its regulation along 170°W in the Pacific sector of the Southern Ocean. Deep-Sea Research II, in press.

JGOFS, 1996. Protocols for the Joint Global Ocean Flux Study (JGOFS) core measurements. JGOFS Report Number 19, Intergovernmental Oceanographic Commission, Bergen, Norway, 170pp.

Johnson, K.S., Gordon, R.M., Coale, K.H., 1997. What controls dissolved iron concentrations in the world ocean? Marine Chemistry 57, 137–161.

Kolber, Z., Zehr, J., Falkowski, P.G., 1988. Effects of growth irradiance and nitrogen limitation on photosynthetic energy conversion in photosystem II. Plant Physiology 88, 923–929.

Kolber, Z., Barber, R.T., Coale, K.H., Fitzwater, S.E., Greene, R.M., Johnson, K.S., Lindley, S., Falkowski, P.G., 1994. Iron limitation of phytoplankton photosynthesis in the equatorial Pacific Ocean. Science 371, 145–149.

Kolber, Z.S., Prasil, O., Falkowski, P.G., 1998. Measurements of variable chlorophyll fluorescence using fast repetition rate techniques: defining methodology and experimental protocols. Biochimica et Biophysica Acta (BBA)—Bioenergetics 1367, 88–106.

Landry, M.R., Barber, R.T., Bidigare, R.R., Chai, F., Coale, K.H., Dam, H.G., Lewis, M.R., Lindley, S.T., McCarthy, J.J., Roman, M.R., Stoecker, D.K., Verity, P.G., White, J.R., 1997. Iron and grazing constraints on primary production in the central equatorial Pacific: an EqPac synthesis. Limnology and Oceanography 42, 405–418.

Landry, M.R., Brown, S.L., Selph, K.E., Abbott, M.R., Letelier, R.M., Christensen, S., Bidigare, R.R., Casciotti, K., 2001. Initiation of the spring phytoplankton increase in the Antarctic Polar Front Zone at 170°W. Journal of Geophysical Research 106, 13903–13915.

Landry, M.R., Selph, K.E., Brown, S.L., Abbott, M.R., Measures, C.I., Vink, S., Allen, C.B., Calbet, A., Christensen, S., Nolla, H., 2002. Seasonal dynamics of phytoplankton in the Antarctic Polar Front region at 170°W. Deep-Sea Research II 49, 1843–1865.

Leonard, C.L., McClain, C.R., Murtugudde, R., Hofmann, E.E., Harding Jr., L.W., 1999. An iron-based ecosystem model of the central equatorial Pacific. Journal of Geophysical Research 104, 1325–1341.

Martin, J.H., Fitzwater, S.E., 1988. Iron deficiency limits phytoplankton growth in the north-east Pacific subarctic. Nature 331, 341–343.

Martin, J.H., Fitzwater, S.E., Gordon, R.M., 1990. Iron deficiency limits phytoplankton growth in Antarctic waters. Global Biogeochemical Cycles 4, 5–12.

Martin, J.H., Coale, K.H., Johnson, K.S., Fitzwater, S.E., Gordon, R.M., Tanner, S.J., Hunter, C.N., Elrod, V.A., Nowicki, J.L., Coley, T.L., Barber, R.T., Lindley, S., Watson, A.J., Van Scoy, K., Law, C.S., 1994. Testing the iron hypothesis in ecosystems of the Equatorial Pacific Ocean. Nature 371, 123–129.

Measures, C.I., Vink, S., 2001. Dissolved Fe in the upper waters of the Pacific sector of the Southern Ocean. Deep-Sea Research II 48, 3913–3941.

Measures, C.I., Yuan, J., Resing, J.A., 1995. Determination of iron in seawater by flow injection analysis using in-line preconcentration and spectrophotometric detection. Marine Chemistry 50, 3–12.

Mitchell, B.G., Brody, E.A., Holm-Hansen, O., McClain, C., Bishop, J., 1991. Light limitation of phytoplankton biomass and macronutrient utilization in the Southern Ocean. Limnology and Oceanography 36, 1662–1677.

Morel, F.M.M., Hudson, R.J.M., Price, N.M., 1991. Limitation of productivity by trace metals in the sea. Limnology and Oceanography 36, 1742–1755.

Morrison, J.M., Gaurin, S., Codispoti, L.A., Takahashi, T., MIllero, F.J., Gardner, W.D., Richardson, M.J., 2001. Seasonal evolution of hydrographic properties in the Antarctic circumpolar current at 170°W during 1997–1998. Deep-Sea Research II 48, 3943–3972.

Olson, R.J., Zettler, E.R., Anderson, O.K., 1989. Discrimination of eukaryotic phytoplankton cell types from light scatter and autofluorescence properties measured by flow cytometry. Cytometry 10, 636–643.

Olson, R.J., Zettler, E.R., DuRand, M.D., 1993. Phytoplankton Analysis Using Flow Cytometry. In: Kemp, P.F., Sherr, B.F., Sherr, E.B., Cole, J.J. (Eds.), Aquatic Microbial Ecology. Lewis Publishers, Boca Raton, pp. 175–186.

Olson, R.J., Chekalyuk, A., Sosik, H.M., 1996. Phytoplankton photosynthetic characteristics from fluorescence induction assays of individual cells. Limnology and Oceanography 41, 1253–1263.

Olson, R.J., Sosik, H.M., Chekalyuk, A.M., 1999. Photosynthetic characteristics of marine phytoplankton from pump-during-probe fluorometry of individual cells at sea. Cytometry 37, 1–13.

Olson, R.J., Sosik, H.M., Shalapyonok, A., 2000. Effects of iron enrichment on phytoplankton in the Southern Ocean during late summer: active fluorescence and flow cytometric analyses. Deep-Sea Research II 47, 3181–3200.

Raven, J.A., 1986. Physiological consequences of extremely small size for autotrophic organisms in the sea. Canadian Bulletin of Fisheries and Aquatic Sciences 214, 1–70.

Sarmiento, J.L., Le Quere, C., 1996. Oceanic carbon dioxide uptake in a model of century-scale global warming. Science 274, 1346–1350.

Shalapyonok, A., Olson, R.J., Shalapyonok, L.S., 2001. Arabian Sea phytoplankton during Southwest and Northeast Monsoons 1995: composition, size structure and biomass from individual cell properties measured by flow cytometry. Deep-Sea Research II 48, 1231–1262.

Smith Jr., W.O., Anderson, R.F., Moore, J.K., Codispoti, L.A., Morrison, J.M., 2000a. The US Southern Ocean Joint Global Ocean Flux Study: an introduction to AESOPS. Deep-Sea Research II 47, 3073–3093.

Smith Jr., W.O., Marra, J., Hiscock, M.R., Barber, R.T., 2000b. The seasonal cycle of phytoplankton biomass and primary productivity in the Ross Sea, Antarctica. Deep-Sea Research II 47, 3119–3140.

Sosik, H.M., Mitchell, B.G., 1994. Effects of temperature on growth, light absorption, and quantum yield in *Dunaliella tertiolecta* (Chlorophyceae). Journal of Phycology 30, 833–840.

Sunda, W.G., Huntsman, S.A., 1997. Interrelated influence of iron, light and cell size on marine phytoplankton growth. Nature 390, 389–392.

van Leeuwe, M.A., Scharek, R., de Baar, H.J.W., de Jong, J.T.M., Goeyens, L., 1997. Iron enrichment experiments in the Southern Ocean: physiological responses of plankton communities. Deep-Sea Research II 44, 189–207.

Zettler, E.R., Olson, R.J., Binder, B.J., Chisholm, S.W., Fitzwater, S.E., Gordon, M.R., 1996. Iron-enrichment bottle experiments in the equatorial Pacific: responses of individual phytoplankton cells. Deep-Sea Research II 43, 1017–1029.